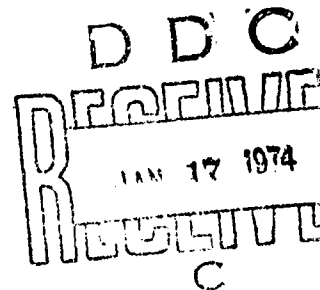RADC-TR-73-365
Technical Report
October 1973

AD772754

INFRARED VIDICON OBSERVATION OF
EXPLODING BALLOON EVENTS

General Electric Company
Space Sciences Laboratory

DDC

IAN 17 1974

C

Rome Air Development Center
Air Force Systems Command
Griffiss Air Force Base, New York

AD-772 754

INFRARED VIDICON OBSERVATION OF EXPLODING BALLOON EVENTS

Fred N. Alyea

General Electric Company

REPORT DOCUMENTATION PAGE	READ INSTRUCTIONS BEFORE COMPLETING FORM

1. REPORT NUMBER	2. GOVT ACCESSION NO.	3. RECIPIENT'S CATALOG NUMBER
RADC-TR-73-365		

4. TITLE (and Subtitle)	5. TYPE OF REPORT & PERIOD COVERED
INFRARED VIDICON OBSERVATIONS OF EXPLODING BALLOON EVENTS	Technical (Interim)
	6. PERFORMING ORG. REPORT NUMBER

7. AUTHOR(s)	8. CONTRACT OR GRANT NUMBER(s)
Dr. Fred N. Alyea	F30602-73-C-0102

9. PERFORMING ORGANIZATION NAME AND ADDRESS	10. PROGRAM ELEMENT, PROJECT, TASK AREA & WORK UNIT NUMBERS
General Electric, Space Sciences Laboratory King of Prussia, PA 19481	62301E-PE 1649-Project 07-Task 03-WUN

11. CONTROLLING OFFICE NAME AND ADDRESS	12. REPORT DATE
Defense Advanced Research Projects Agency 1400 Wilson Blvd. Arlington, VA 22209	October 1973
	13. NUMBER OF PAGES
	35 45

14. MONITORING AGENCY NAME & ADDRESS(if different from Controlling Office)	15. SECURITY CLASS. (of this report)
Rome Air Development Center (OCSE) Griffiss Air Force Base, New York 13441	UNCLASSIFIED
	15a. DECLASSIFICATION/DOWNGRADING SCHEDULE
	N/A

16. DISTRIBUTION STATEMENT (of this Report)

Approved for public release; distribution unlimited.

17. DISTRIBUTION STATEMENT (of the abstract entered in Block 20, if different from Report)

Same

18. SUPPLEMENTARY NOTES   Monitored by:
Jospeh J. Simons (OCSE)
RADC/GAFB, NY 13441
AC 315 330-3055

19. KEY WORDS (Continue on reverse side if necessary and identify by block number)

Vidicons
Infrared
Exploding Balloons

20. ABSTRACT (Continue on reverse side if necessary and identify by block number)

Predictions of the IR radiation produced by the debris of stoichiometric $CO/O_2/H_2O$ and CH_4/O_2 explosion mixtures have been made. The calculation considered optical thickness effects as well as spatial and temporal variations of the major species, CO_2 and H_2O and temperature. The results show that the spectral intensity is a strong function of wavelength and determined in part by the optical thickness of the cloud. The predictions have been applied to select appropriate filters for an infrared vidicon sensor system which will be used for observation of balloons exploded in the field.

DD FORM 1473   EDITION OF 1 NOV 65 IS OBSOLETE
1 JAN 73

INFRARED VIDICON OBSERVATION OF
EXPLODING BALLOON EVENTS

Dr. Fred N. Alyea

Contractor: General Electric Company, Space Sciences Lab.
Contract Number: F30602-73-C-0102
Effective Date of Contract: 16 February 1973
Contract Expiration Date: 31 December 1973
Amount of Contract: $131,065.00
Program Code Number: 3E20

Principal Investigator: Dr. Fred N. Alyea
                Phone: 215 962-6038

Project Engineer: Joseph J. Simons
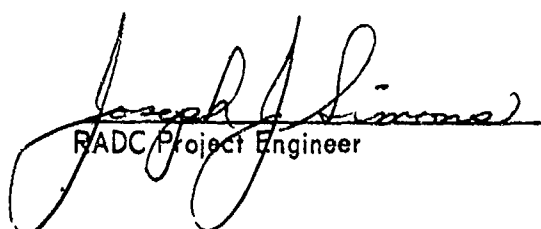   Phone: 31   30-3055

iѡ

PUBLICATION REVIEW

This technical report has been reviewed and is approved.

RADC Project Engineer

iv

ACKNOWLEDGEMENT

iD

SUMMARY

Predictions of the IR radiation produced by the debris of stoichiometric $CO/O_2/H_2O$ and CH_4/O_2 explosion mixtures have been made. The calculation considered optical thickness effects as well as spatial and temporal variations of the major species, CO_2 and H_2O and temperature. The results show that the spectral intensity is a strong function of wavelength and is determined in part by the optical thickness of the cloud. The predictions have been applied to select appropriate filters for an infrared vidicon sensor system which will be used for observation of balloons exploded in the field.

TABLE OF CONTENTS

LIST OF FIGURES

LIST OF FIGURES Cont'd.

LIST OF TABLES

vi

I. INTRODUCTION

The Air Force Weapons Laboratory (AFWL) is conducting a series of field experiments to evaluate the flow characteristics of balloon explosions.[1] A primary diagnostic for these events will be an infrared vidicon sensor system operated by the General Electric Company Space Sciences Laboratory (GE-SSL) under sponsorship of the Advanced Research Projects Agency (ARPA). This report presents design predictions for these measurements.

The detonable mixtures under consideration include stoichiometric mixtures of $CO/O_2/H_2O$ and CH_4/O_2. The major products of the explosion, CO_2 and H_2O, exhibit strong infrared signatures between 2.5 and 3.5 microns. In fact, the debris of the explosion is optically thick in this spectral region. Consequently, a prediction of the expected emission from the explosion must solve the radiative transfer equation along a line-of-sight passing through the disturbed region. This will enable the selection of appropriate spectral filters to optimize the measurements and will define the desired dynamic range of the sensor system.

The following sections describe the methodology used for the radiation predictions, present results computed for the two mixtures under consideration and recommend instrument parameters for the field experiments.

1

II. DISCUSSION OF THEORY

II.1   INTRODUCTION

The detonation products of stoichiometric mixtures of $CO/O_2/H_2O$ and CH_4/O_2 contain large quantities of H_2O and CO_2. In addition, trace amounts of CO, OH, H_2 and various hydrocarbons are present.[2] The infrared spectra of the major species are particularly strong from 2.5 to 3.5 microns as is shown by Figures 1 and 2. This in conjunction with the expected concentrations leads to the conclusion that the infrared signature of the explosion will be governed by the major species. Thus, only emission from H_2O and CO_2 is considered in the present calculations.

A realistic prediction of the expected intensity of the explosion debris must consider the temperature and concentration variation with time and position as well as optical thickness effects. The radiative transfer model, which accounts for the above phenomenology, is discussed below while that of the debris distribution is considered in the subsequent section.

II.2   RADIATIVE TRANSFER MODEL

The monochromatic radiative transfer equation along a ray passing through the disturbed environment to the sensor is given by:[3]

$$\frac{dI_\nu}{ds} = \epsilon_\nu - I_\nu \alpha_\nu \qquad (1)$$

where:

I_ν = spectral intensity (watts/cm^2-ster-cm^{-1})

s = distance along ray (cm)

ϵ_ν = spectral emission coefficient, (watts/cm^3-ster-cm^{-1}) a function of s

α_ν = spectral absorption coefficient, (1/cm) a function of s
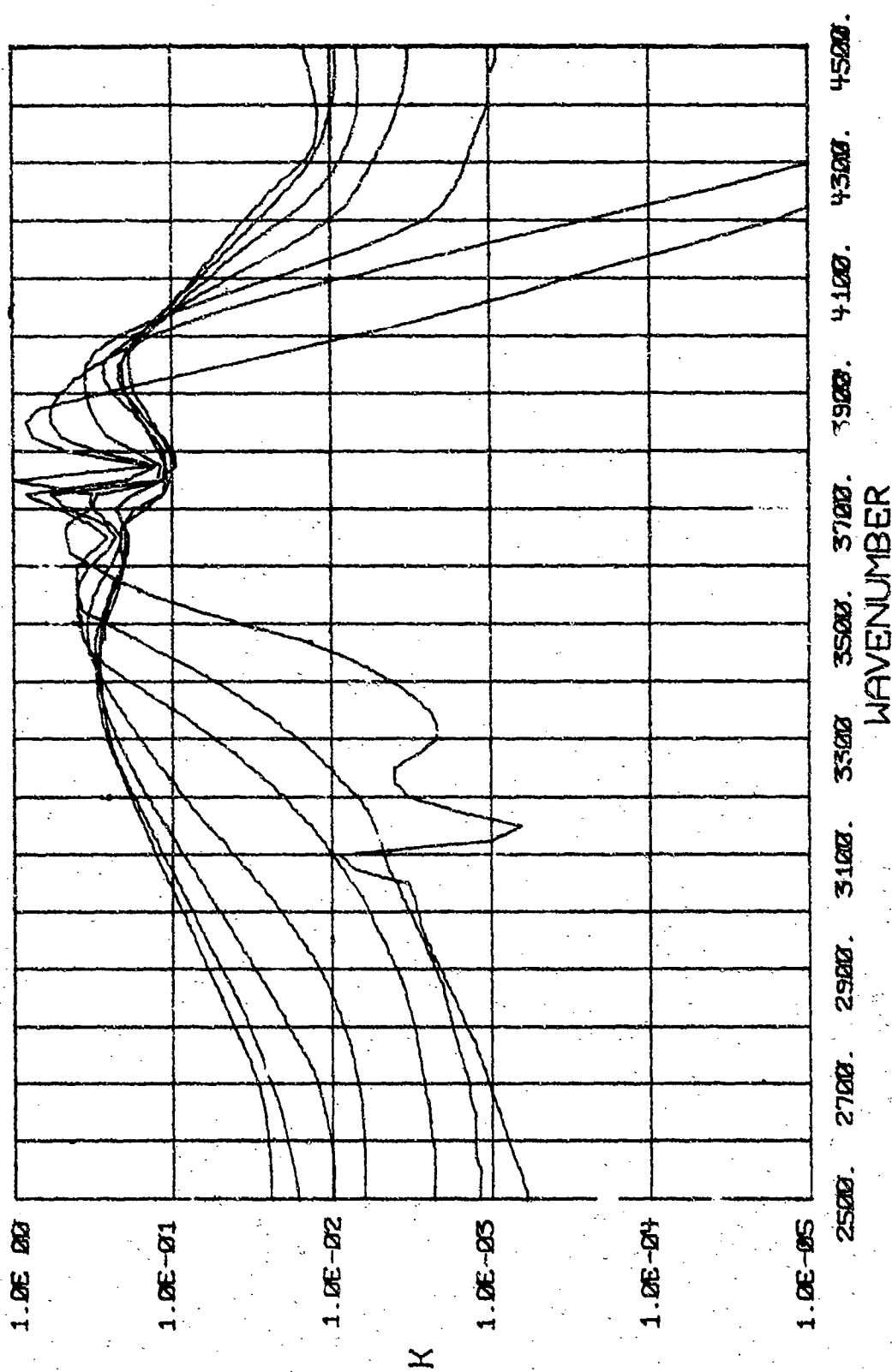
Figure 1. Absorption Coefficients of Water Taken from Reference 5. The Temperature Variation is 3000, 2500, 2000, 1500, 1000, 600 and 300°K for Curves Going from Top to Bottom.
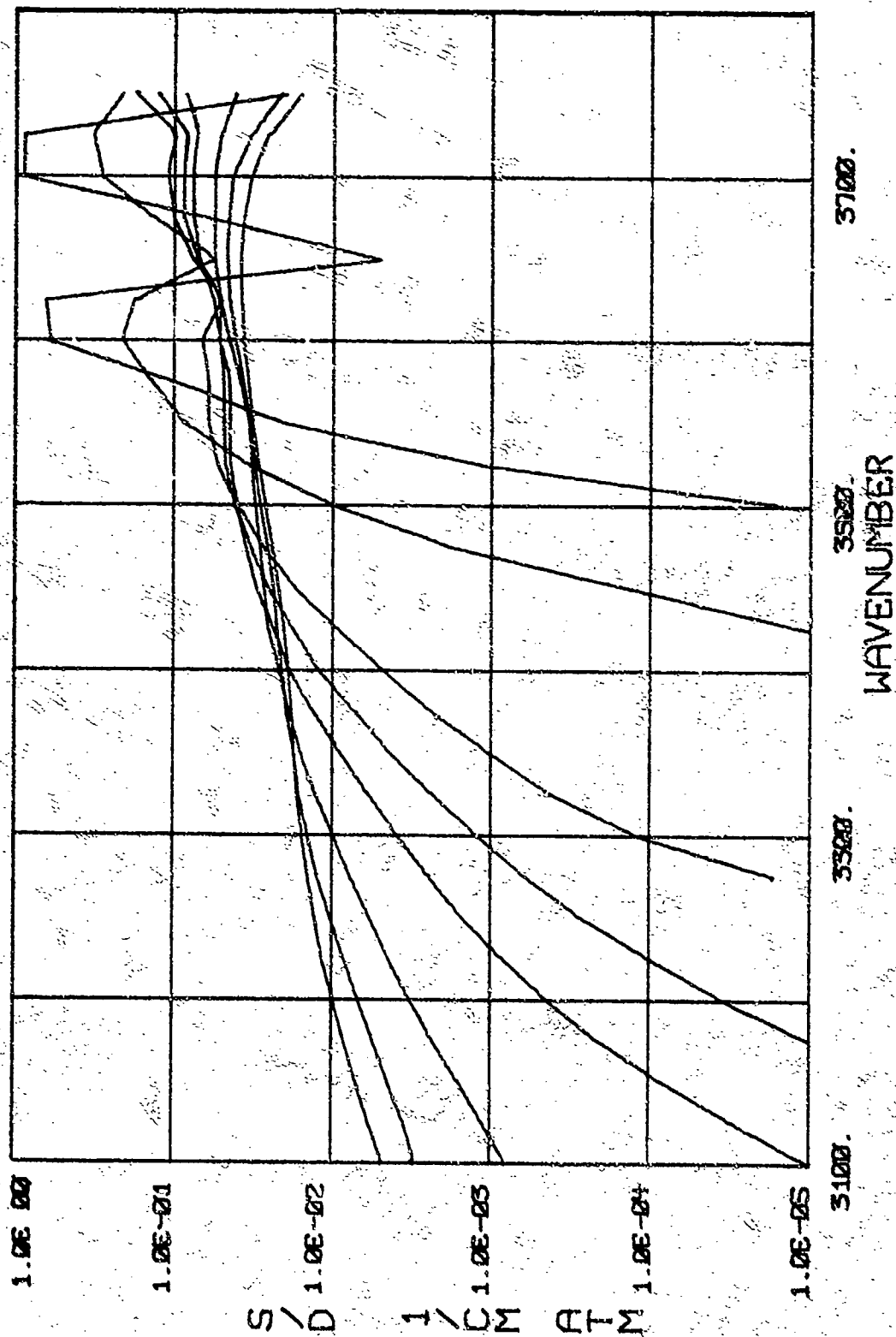
Figure 2. Absorption Coefficients of Carbon Dioxide Taken from Reference 6. The Temperature Variation is 3600, 3000, 2400, 1800, 1500, 1200, 600 and 300 k for Curves Going From Top to Bottom.

4

Formal integration of Equation (1) results in:

$$I_\nu(z) = I_{o,\nu} e^{-\int_o^z \alpha_\nu ds''} + \int_o^z \varepsilon_\nu e^{-\int_{s'}^z \alpha_\nu ds''} ds' \qquad (2)$$

where:

I_o = background intensity (watts/cm^2-ster-cm^{-1}).

In practice, Equation (2) has been integrated numerically using Simpson's rule, a procedure which optimizes efficiency and minimizes error.[4]

The properties ε_ν and α_ν are functions of position and wavenumber which must be evaluated prior to integration.

Ideally, Equation (2) should be solved as a function of wavenumber with a resolution sufficient to describe the details of self-absorbed, overlapping rotational lines. However, for the case of H_2O and CO_2, the basic spectroscopic information (line strengths and energy levels) is not available for the hot bands. Consequently, the absorption and emission coefficients have been approximated by a statistical model[5] using 25 cm^{-1} resolution. The absorption coefficients for H_2O, shown in Figure 1, were taken from Ferriso, et al and are related to α_ν by:

$$\alpha_{\nu,H_2O} = \frac{k_\nu P_{H_2O}}{1 + (k_\nu P_{H_2O}/4a_\nu)^{1/2}} \qquad (3)$$

where:

k_ν = spectral absorption coefficient from Ref. 5 (cm^{-1}-atm^{-1})

P_{H_2O} = partial pressure of water vapor (atm)

a_ν = fine structure term (cm^{-1})

The fine structure term is proportional to the local mean value of the ratio of the collision half-width to the line spacing, γ/d.

5

The value for this parameter recommended by Ferriso, et al, is given by:

$$a_\nu = \frac{0.5}{d_\nu} \left(\frac{300}{T}\right)^{1/2} \left[P_{H_2O} \left(\left(\frac{300}{T}\right)^{1/2} + 0.1 \right) + \right.$$

$$\left. 0.1593(1 - P_{H_2O}) \right] \tag{4}$$

where:

    T = local temperature $^\circ$K

    $d_\nu = \exp(-0.0016\ T + 1.21)$ $\tag{5}$

In the case of CO_2, fine structure parameters were not readily available. Consequently, the theoretical absorption coefficients of Malkmus[6] shown in Figure 2 have been used.

$$\alpha_{\nu,CO_2} = \frac{S}{d}\ P_{CO_2} \tag{6}$$

where:

    $\frac{S}{d}$ = mean spectral absorption coefficient from Ref. 6 (cm^{-1}-atm^{-1}).

    P_{CO_2} = partial pressure of CO_2 (atm).

The total absorption coefficient is now given by:

$$\alpha_\nu = \alpha_{\nu,H_2O} + \alpha_{\nu,CO_2} \tag{7}$$

and the emission coefficient is computed using Kirchoff's law:

$$\varepsilon_\nu = \alpha_\nu\ B(T,\nu) \tag{8}$$

where:

    $B(T,\nu)$ = black body function (watts/cm^2-ster-cm^{-1})

6

The computational procedure uses Equations (3) through (8) and the data of Figures 1 and 2 to evaluate α_ν and ϵ_ν from a knowledge of the temperature and the partial pressures of CO_2 and H_2O. Numerical integration of Equation (2) is then accomplished using the sky background intensities shown in Figure 3 as initial conditions.[7]

II.3   Flow Field of Explosion Debris

The properties of the flow field associated with the debris of the balloon explosion were obtained from the computations described in Reference 1. A one-dimensional Langrangian code (SAP) with spherical symmetry was used to burn a CH_4/O_2 mixture. The output data then, supplied initial conditions for a time dependent, cylindrically symmetric model for compressible, inviscid, non-conducting laminar flows (HULL). The resulting flow field provided distributions of temperature, density and the ratio of entrained air to explosion debris as a function of time and position. These data were further reduced by taking a ray perpendicular to the ground passing through the hottest point of the disturbed environment.[8] The resulting temperature profiles along this ray for three values of time are shown in Figure 4.

The ratio of entrained air to explosion debris has been used to obtain partial pressures of the major species, H_2O and CO_2. It was assumed that ambient air contained 3.1×10^{-2} and 1.01×10^{-1} mole percent of CO_2 and H_2O, respectively. The latter figures being based on 60% relative humidity at $60°F$.[8] The partial pressures of CO_2 and H_2O are then given by:

$$P_{H_2O} = 1.01 \times 10^{-3} + y_d \left(X_{H_2O} - 1.01 \times 10^{-3} \right)$$

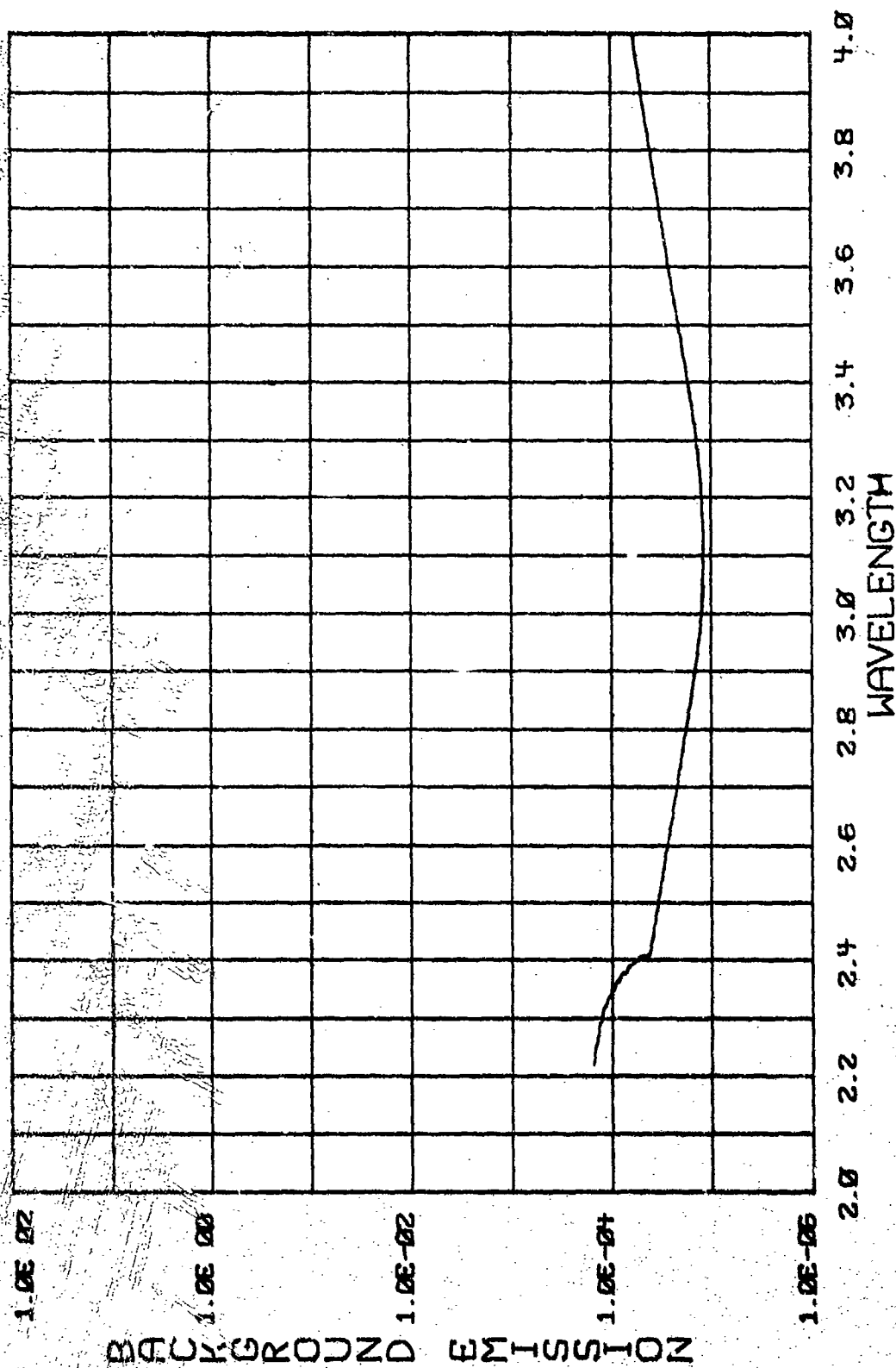$$P_{CO_2} = 3.1 \times 10^{-4} + y_d \left(X_{CO_2} - 3.1 \times 10^{-4} \right) \tag{9}$$

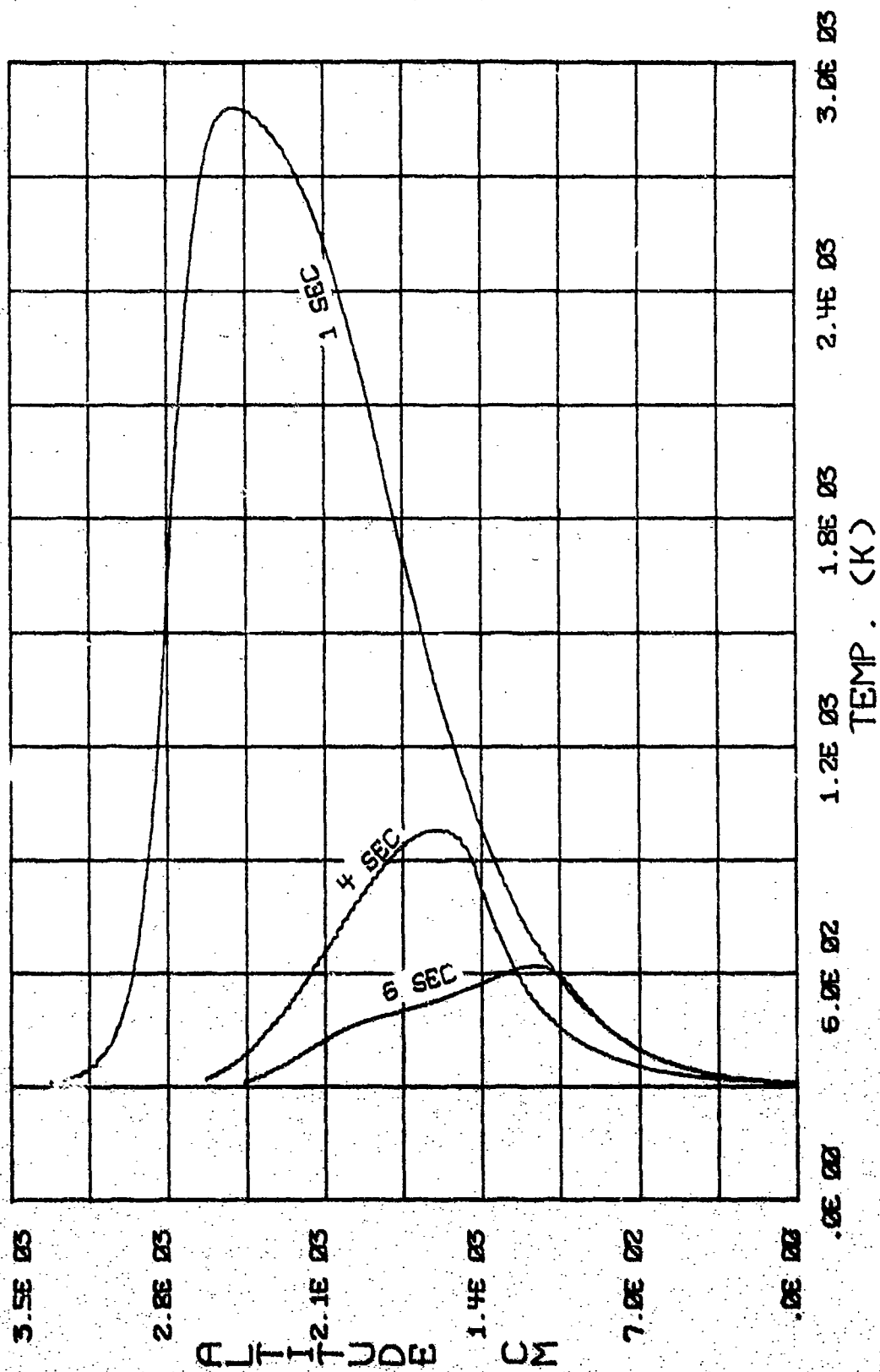Figure 3. Background Spectral Intensity

Figure 4. Temperature Profiles of the Debris as a Function of Time.

where:

X_{H_2O} = mole fraction of H_2O in detonated mixture

X_{CO_2} = mole fraction of CO_2 in detonated mixture,

and y_d, the mole fraction of debris in air is computed from:

$$y_d = \frac{1}{1 + \frac{M_dR}{29}} \qquad (10)$$

where:

M_d = molecular weight of debris mixture

R = ratio of air to debris in grams/gram from HULL calculations.

Equation (9) is valid at low temperatures. However, at early times, CO_2 and H_2O are partially dissociated. Consequently, the partial pressures of these species are somewhat reduced. This has been taken into account using the equilibrated reactions:

$$CO_2 = CO + 1/2 \ O_2$$
$$H_2O = OH + 1/2 \ H_2 \qquad (11)$$
$$OH = 1/2 \ H_2 + 1/2 \ O_2$$
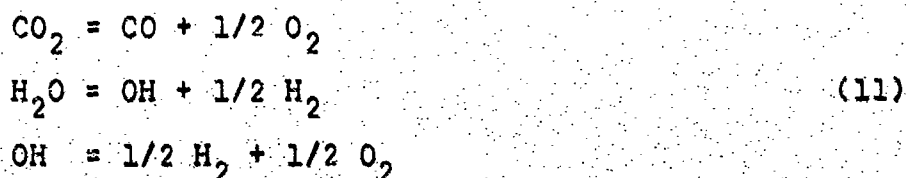
The resulting partial pressures used for the computations are shown as a function of time and position in Figures 5-8. The assumed debris compositions are shown in Table I.

1.0E 00

1.0E-01

1.0E-02

1.0E-03

CO2 PARTIAL PRESS ATM

.0E 00   7.0E 02   1.4E 03   2.1E 03   2.8E 03   3.5E 03

ALTITUDE CM

.1 SEC

4 SEC

6 SEC
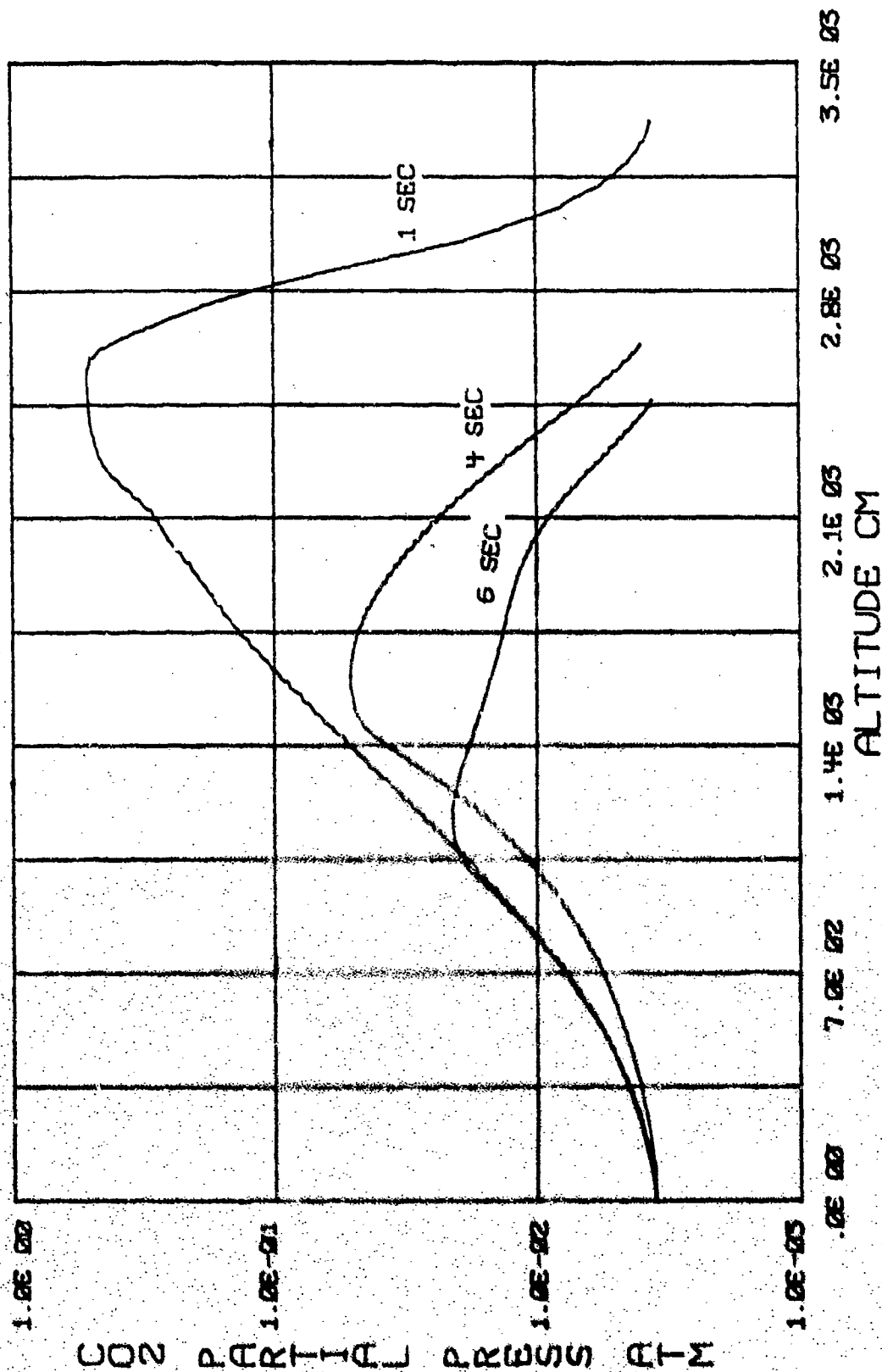
Figure 5. CO_2 Partial Pressure Profiles for $CO/O_2/H_2O$ Explosions

11
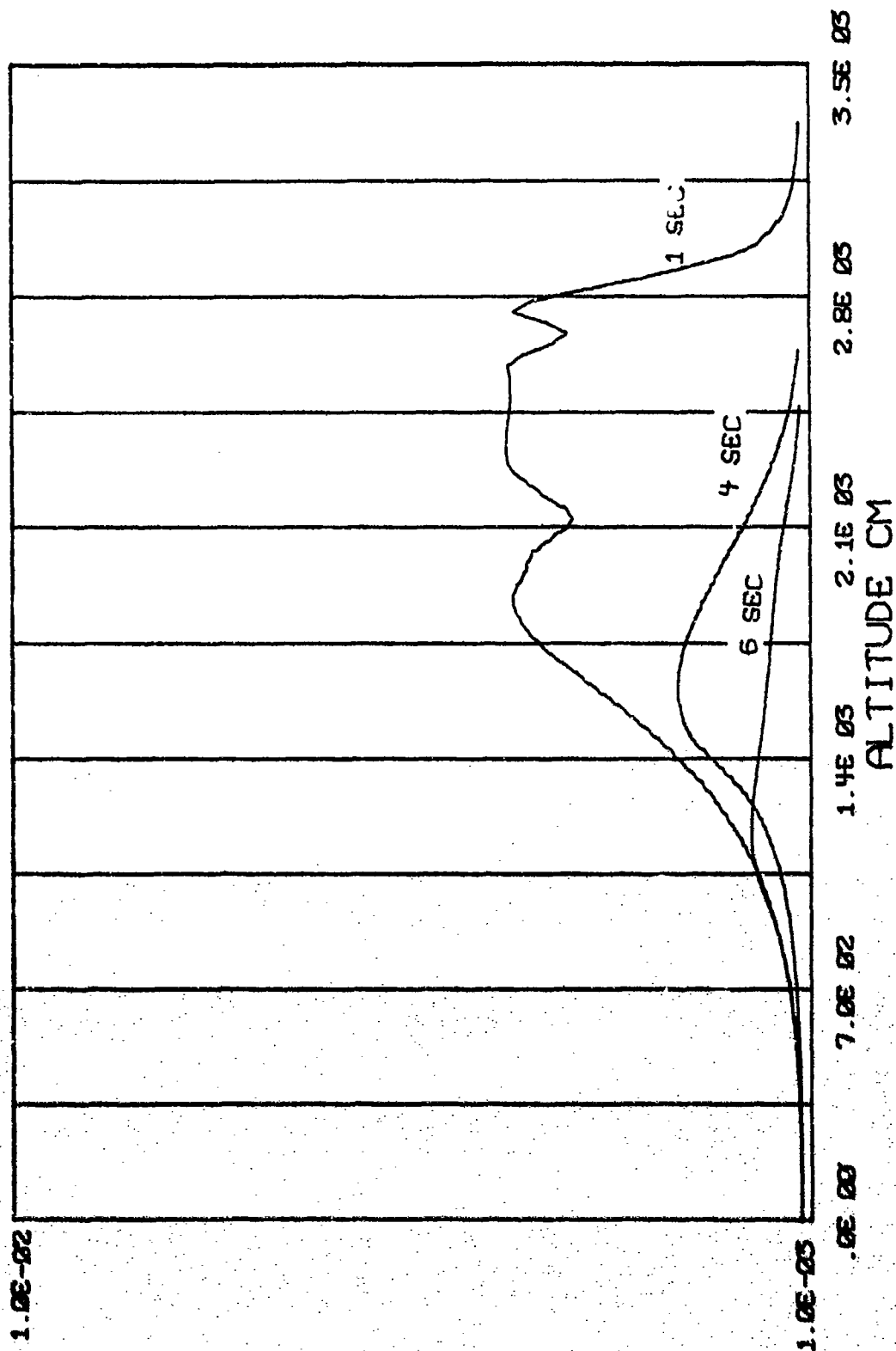
Figure 6. H_2O Partial Pressure Profiles for $CO/O_2/H_2O$ Explosions

Figure 7. CO_2 Partial Pressure Profiles for CH_4/O_2 Explosions.
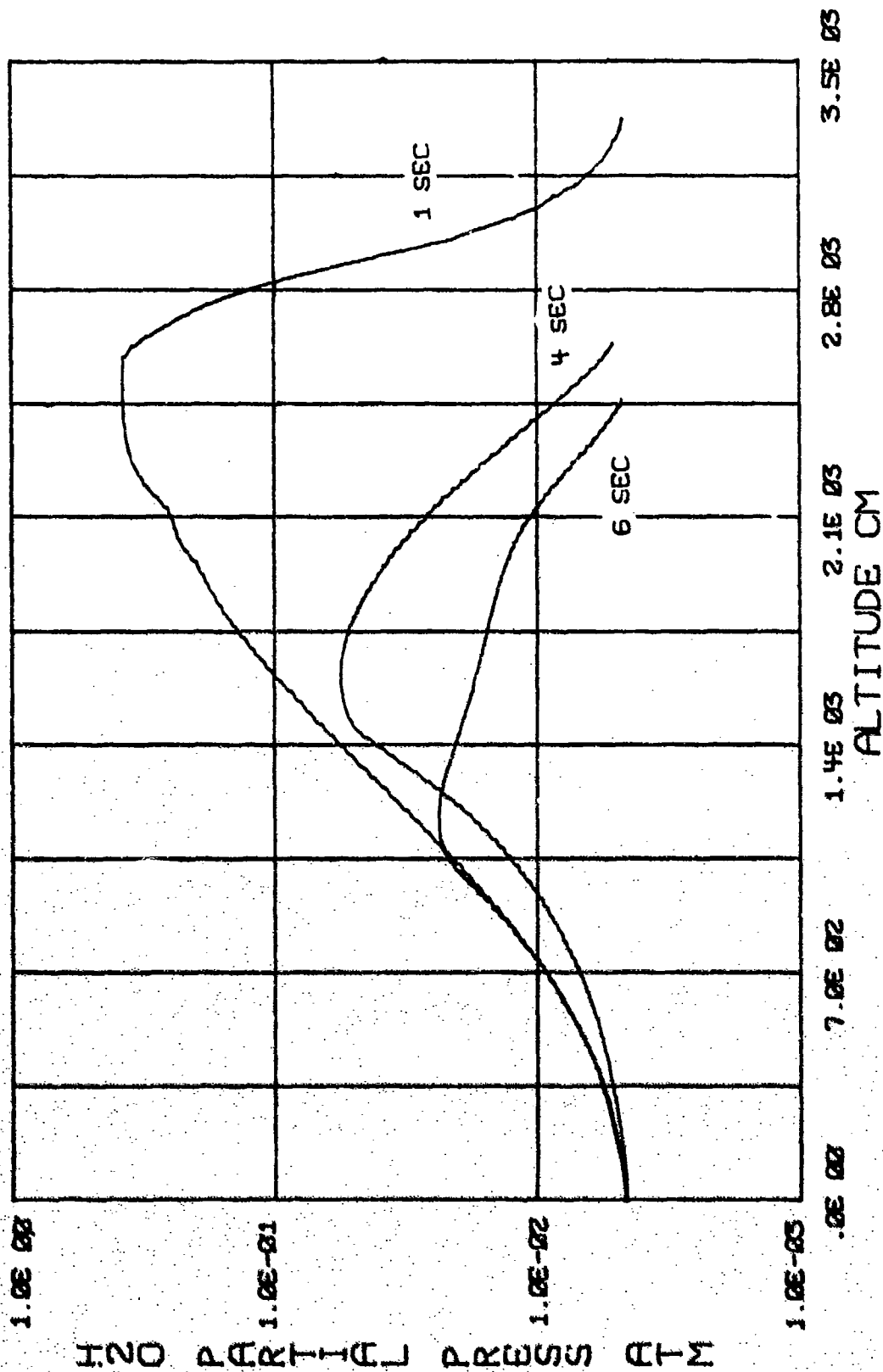
Figure 6. H_2O Partial Pressure Profiles for CH_4/O_2 Explosions.

TABLE I

DEBRIS COMPOSITIONS

MIXTURE	MOLE FRACTION	
	CO_2	H_2O
$CO/O_2/H_2O$	0.99	0.01
CH_4/O_2	0.333	0.667

III. DISCUSSION OF RESULTS

III.1 INTRODUCTION

The calculational procedure discussed in the previous section
has been applied for the prediction of the emission produced by
detonating mixtures of $CO:O_2:H_2O = 1:0.5:0.01$ and $CH_4:O_2 = 1:3$. The
results of these computations apply along a ray perpendicular to the
ground and passing through the peak temperature point of the disturbed
environment. Three times; 1, 4 and 6 seconds were considered. The
details of the radiation field are presented in the following sections.
Then, recommendations for the IR vidicon field experiments are out-
lined.

III.2 EMISSION PREDICTIONS

The spectral intensity predicted for the CO and CH_4 detonations
is shown in Figures 9-11 and 12-14, respectively. It is noted that
the CO_2 absorption coefficient (see Figure 2) was taken as zero for
wavelengths greater than 3.225 microns. This causes a jump in the
spectrum which is particularly noticable in Figure 9. Difficulties
arising from this assumption are not anticipated because the field
measurements against CO target balloons will not be taken at wave-
lengths greater than 3.2 microns.

Examination of the spectral intensities indicates, in general,
a strong variation with time. However, the band centers are strongly
self-absorbed and the intensity is controlled by optical thickness
effects. For methane, the thickest regions of the spectrum exhibit
no dependence with time while for CO_2 the variation is about a factor
of three. In contrast, the wings of the bands change by as much as
five to six orders of magnitude over the same time period. These
results are shown in Figures 15 and 16 where the dynamic range (ratio
of emission to background) is plotted as a function of wavelength.

16

Figure 9. Spectral Intensity for $CO/O_2/H_2O$ Explosion. Time = 1 Second.

17

Figure 10. Spectral Intensity for $CO/O_2/H_2O$ Explosion. Time = 4 Seconds.

18

Figure 11. Spectral Intensity for $CO/O_2/H_2O$ Explosion. Time = 6 Seconds.

19

Figure 12. Spectral Intensity for CH_4/O_2 Explosion. Time = 1 Second.
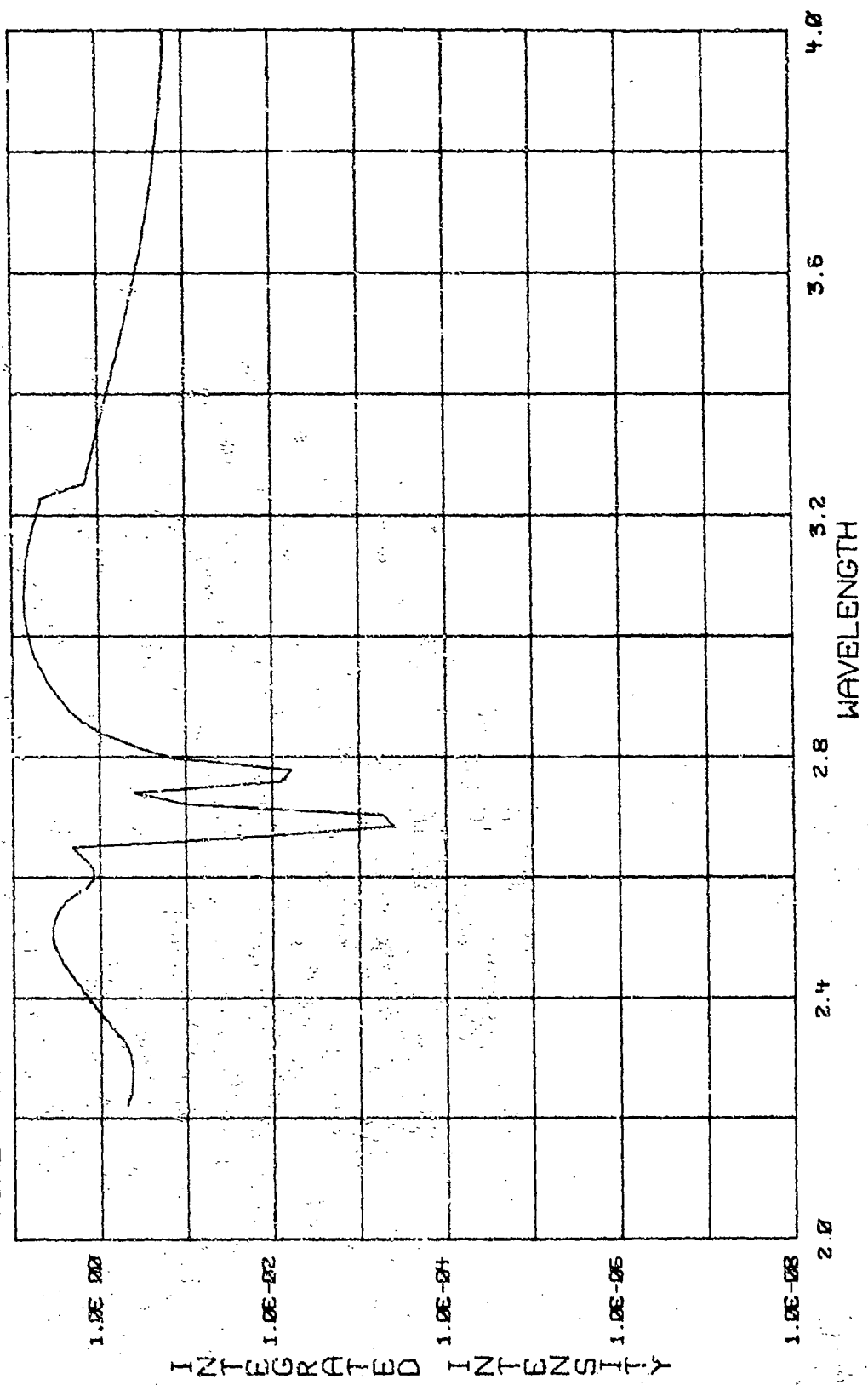
20

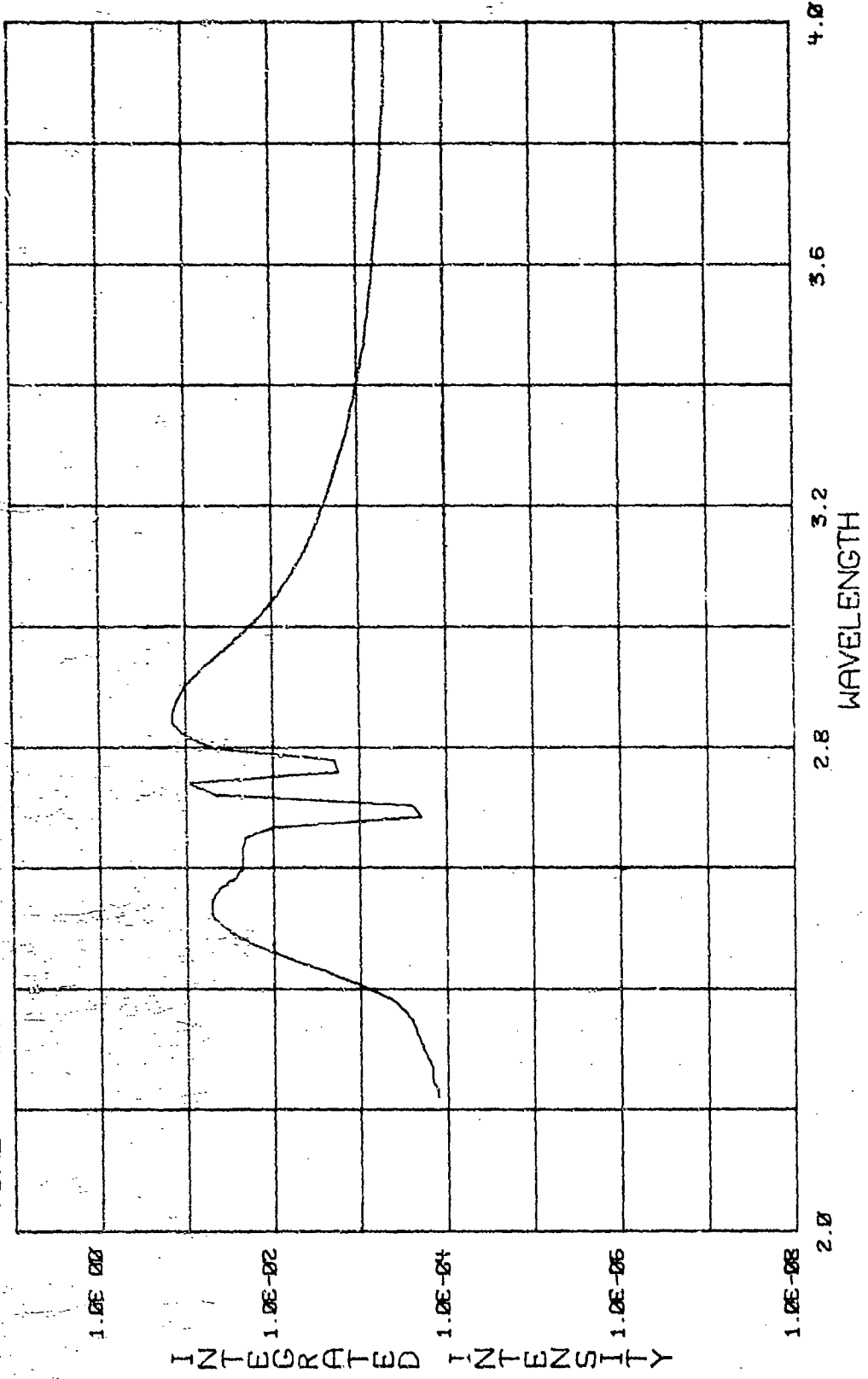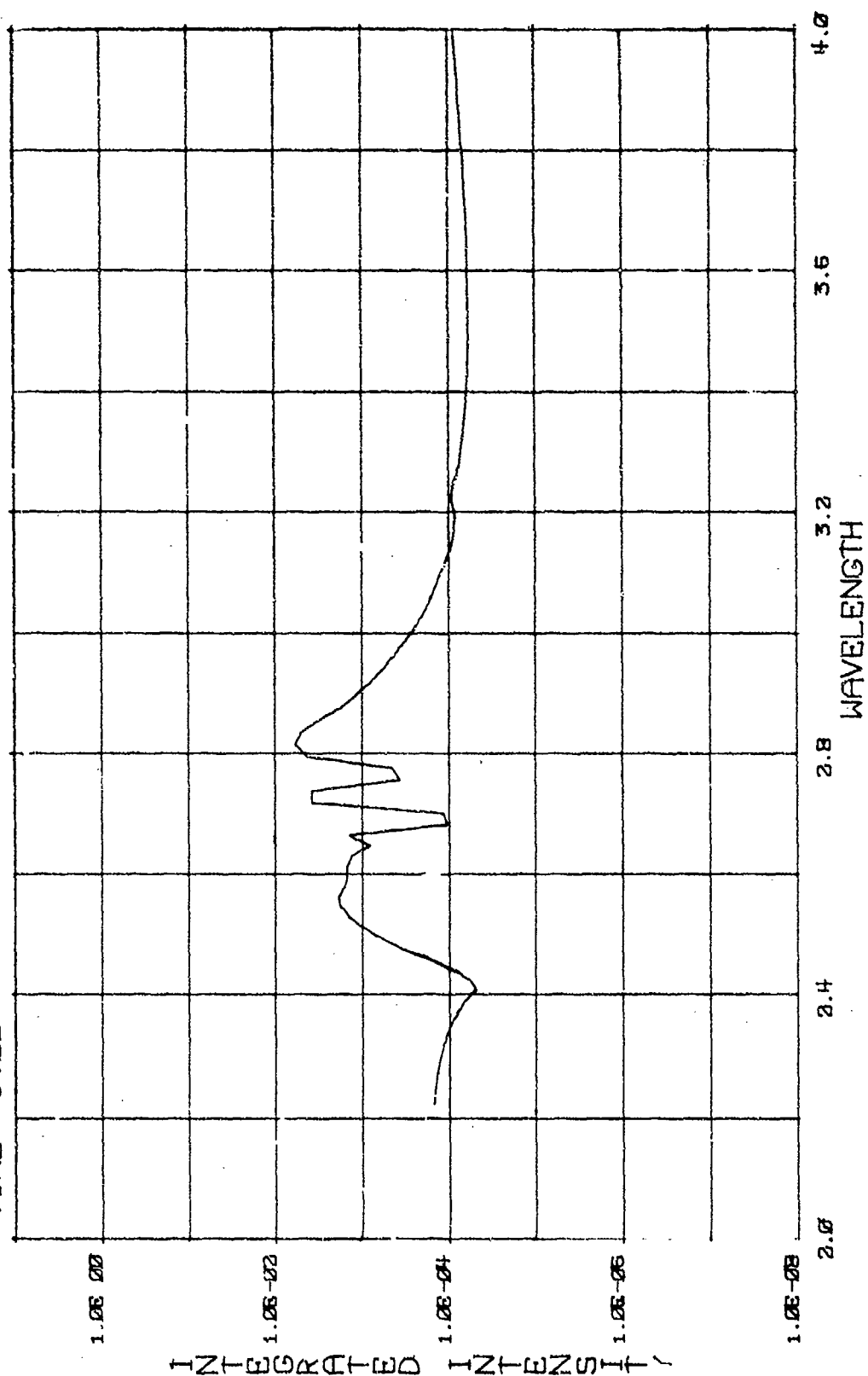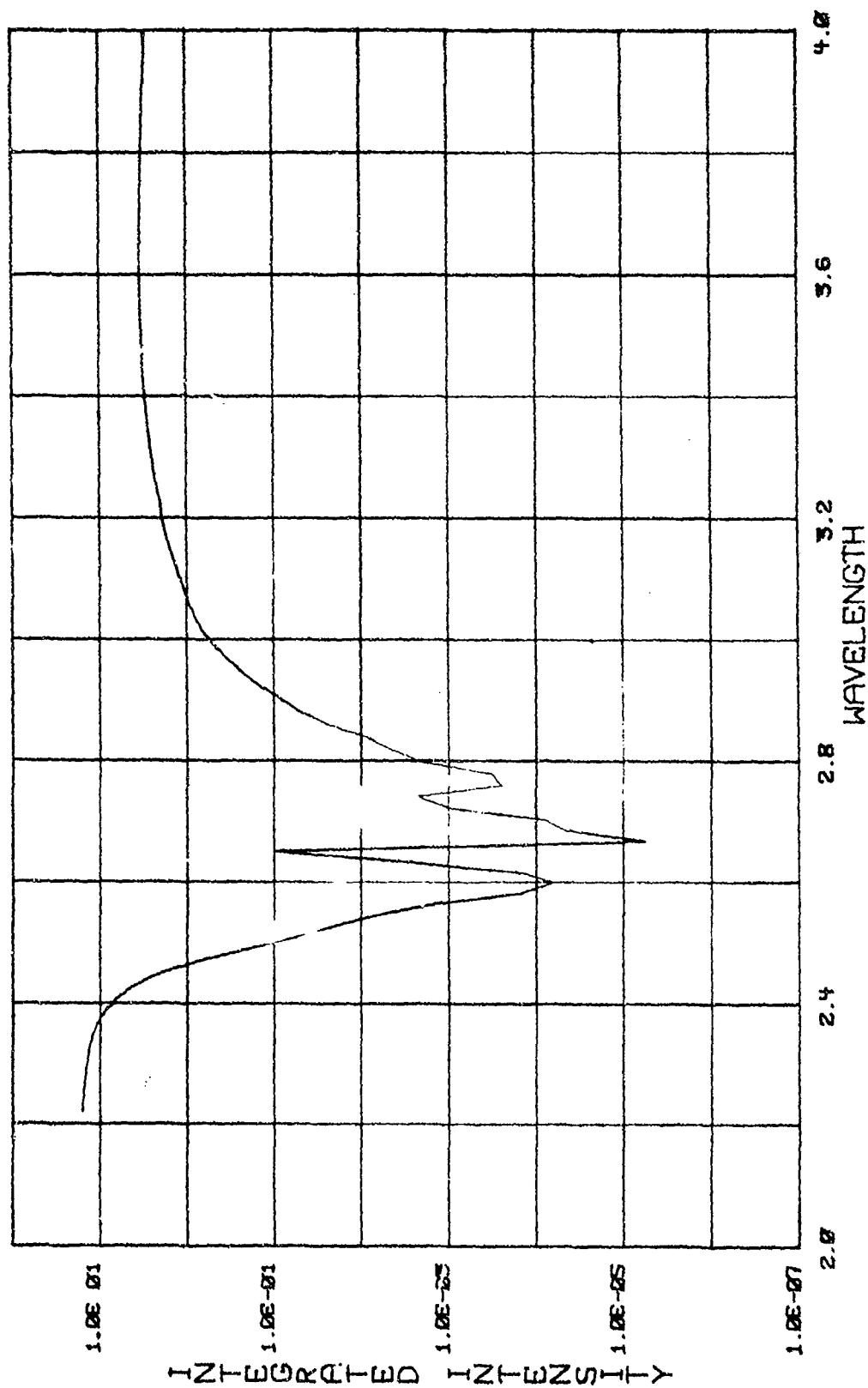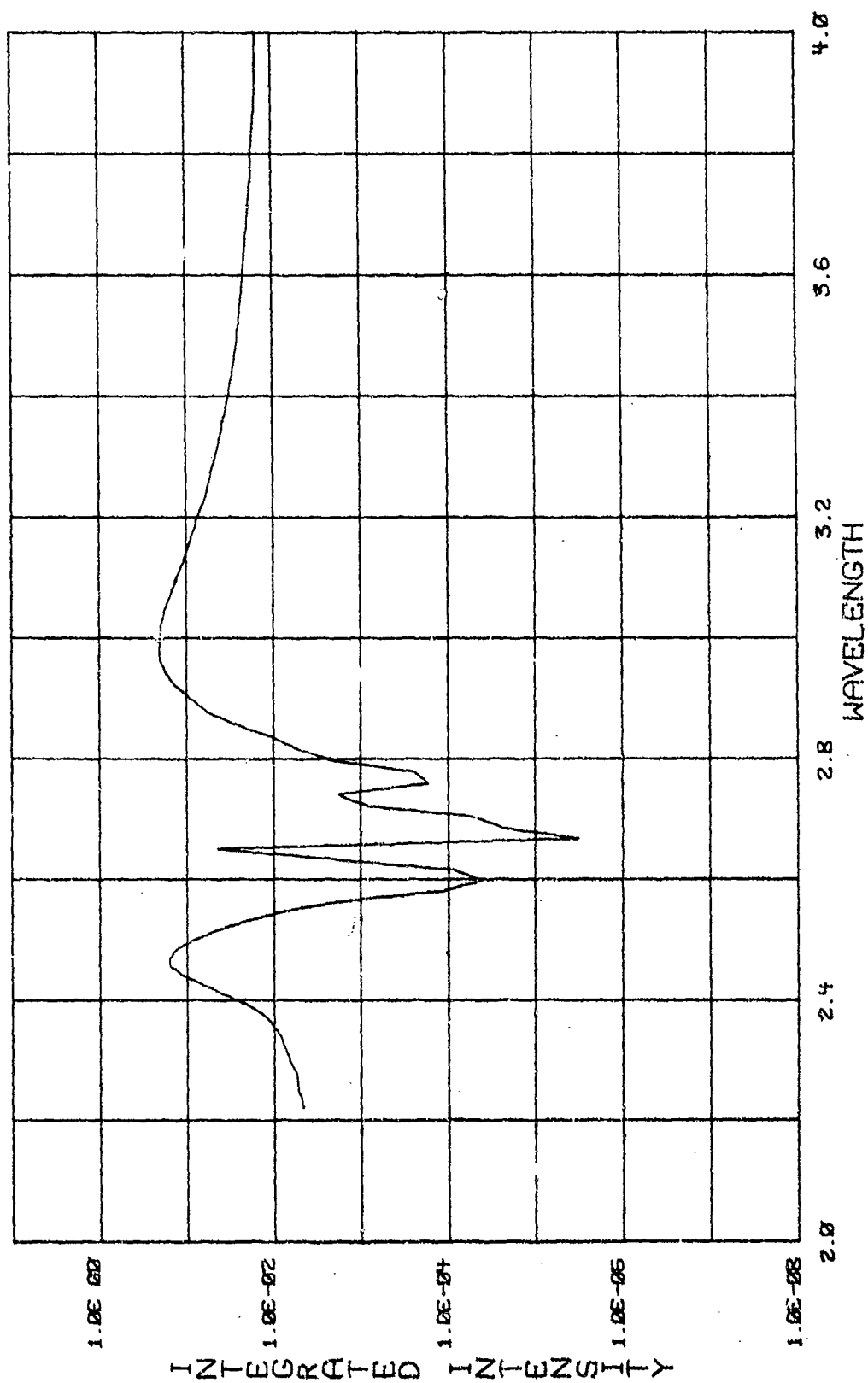Figure 13. Spectral Intensity for CH_4/O_2 Explosion. Time = 4 Seconds.

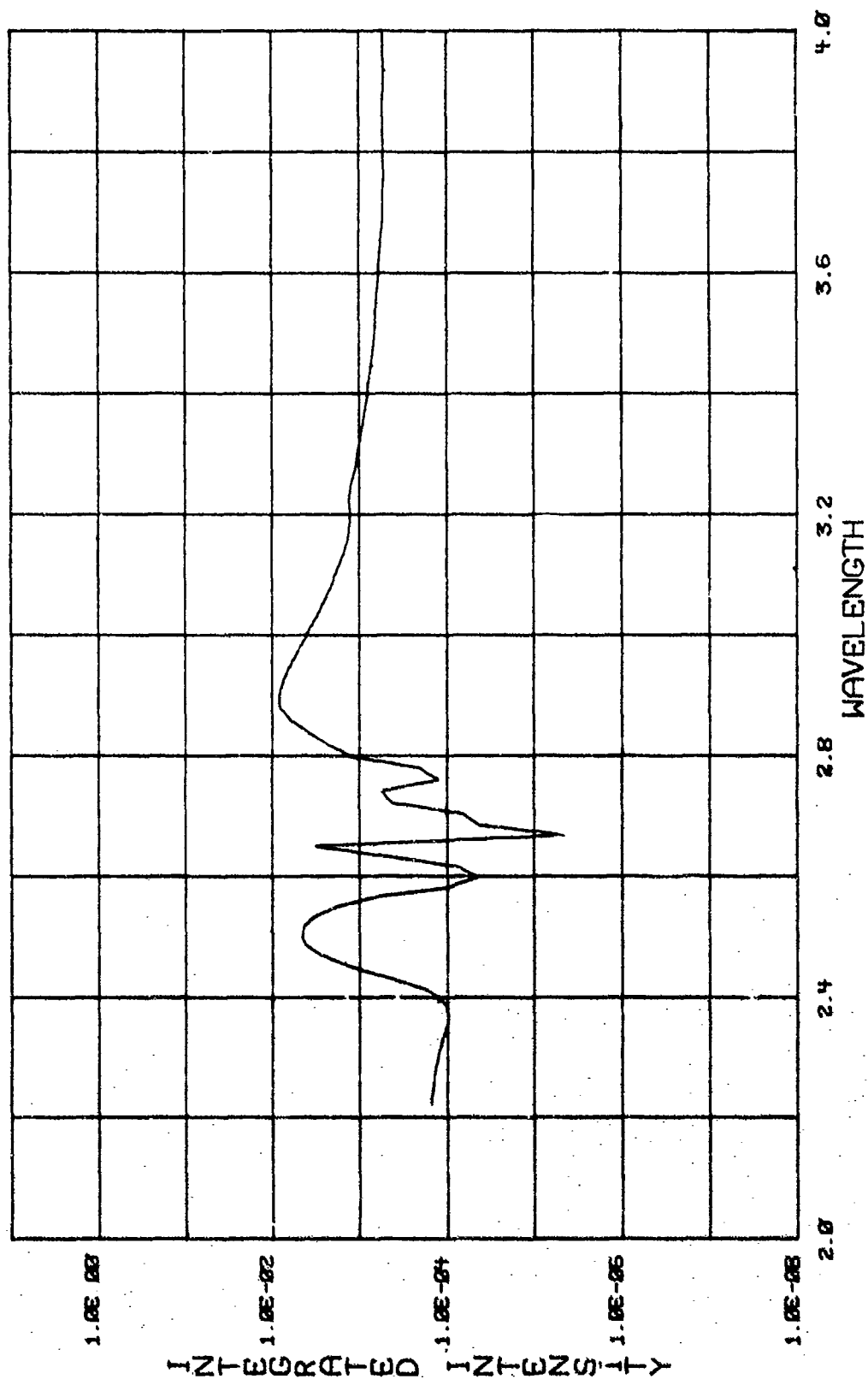BALLOON EXPLOSION CO2 + WATER EMISSION SPECTRA

TIME =6.00

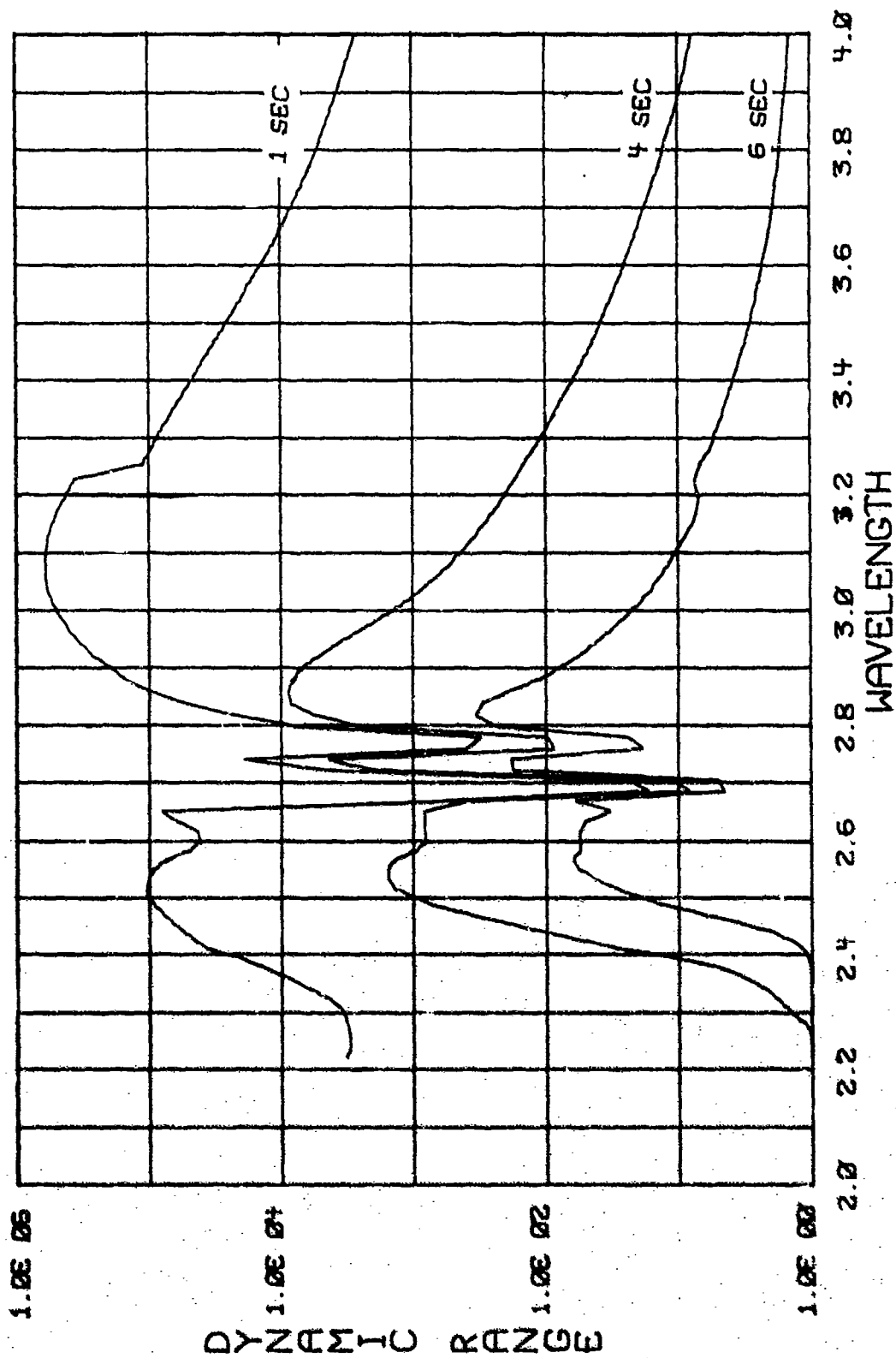Figure 14. Spectral Intensity for CH_4/O_2 Explosion. Time = 6 Seconds.

Figure 15. Spectral Dynamic Range = Spectral/Background Intensity for $CO/O_2/H_2O$ Explosions.
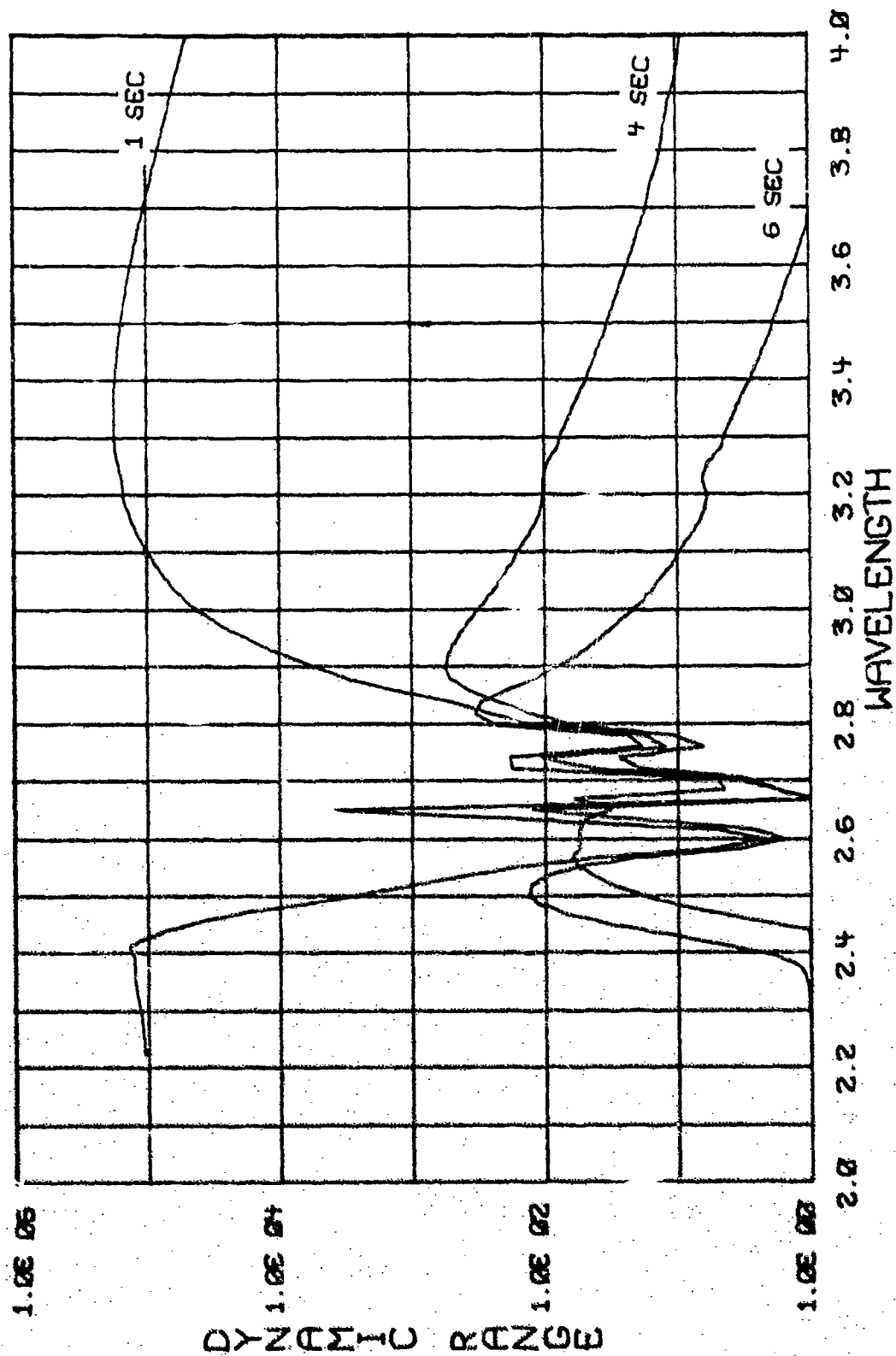
23

Figure 16. Spectral Dynamic Range = Spectral/Background Intensity for CH_4/O_2 Explosions.

24

The behavior described above can be explained by noting that the cool outer region of the debris cloud absorbs radiation produced by the hot central core. The degree of absorption depends on optical depth from the source to the observer. As the wavelength varies, the optical depth changes, thus, modifying the absorption. This, in turn, alters that region of the cloud which is observed. To illustrate these points, the relative contribution to the observed intensity is plotted as a function of distance along the ray in Figure 17. The wavelength and the optical thickness to the peak temperature point are shown as parameters (the integral under the curves is directly proportional to the observed intensity). At 2.86 microns, the debris is very thick and the observed emission originates in the outer cool region of the cloud. As the wavelength increases, the optical thickness decreases and the emission is more characteristic of the hot inner core. At later times when the debris has been diluted by the entrainment process, only the band centers are fully absorbed. The wings of the band are thin and the relative intensity distribution becomes independent of wavelength as is shown in Figure 18.

Figures 19 and 20 present the optical thickness from the edge of the disturbed region to the peak temperature point as a function of time and wavelength. The $CO/O_2/H_2O$ debris is optically thin for wavelengths less than 2.65 microns and greater than 3.15 microns, i.e., that region where CO_2 absorption is not significant. On the other hand, the CH_4/O_2 mixture is optically thick for all wavelengths considered at time = 1 sec. For later times the cloud becomes optically thin at wavelengths less than 2.45 microns and greater than 3 microns.

In summary, predictions have been made for the emission produced by the explosion debris of $CO/O_2/H_2O$ and CH_4/O_2 mixtures. The radiation is significantly effected by absorption. Emission at the band centers where the cloud is optically thick, originates in a region which is removed from the peak temperature point. The relative
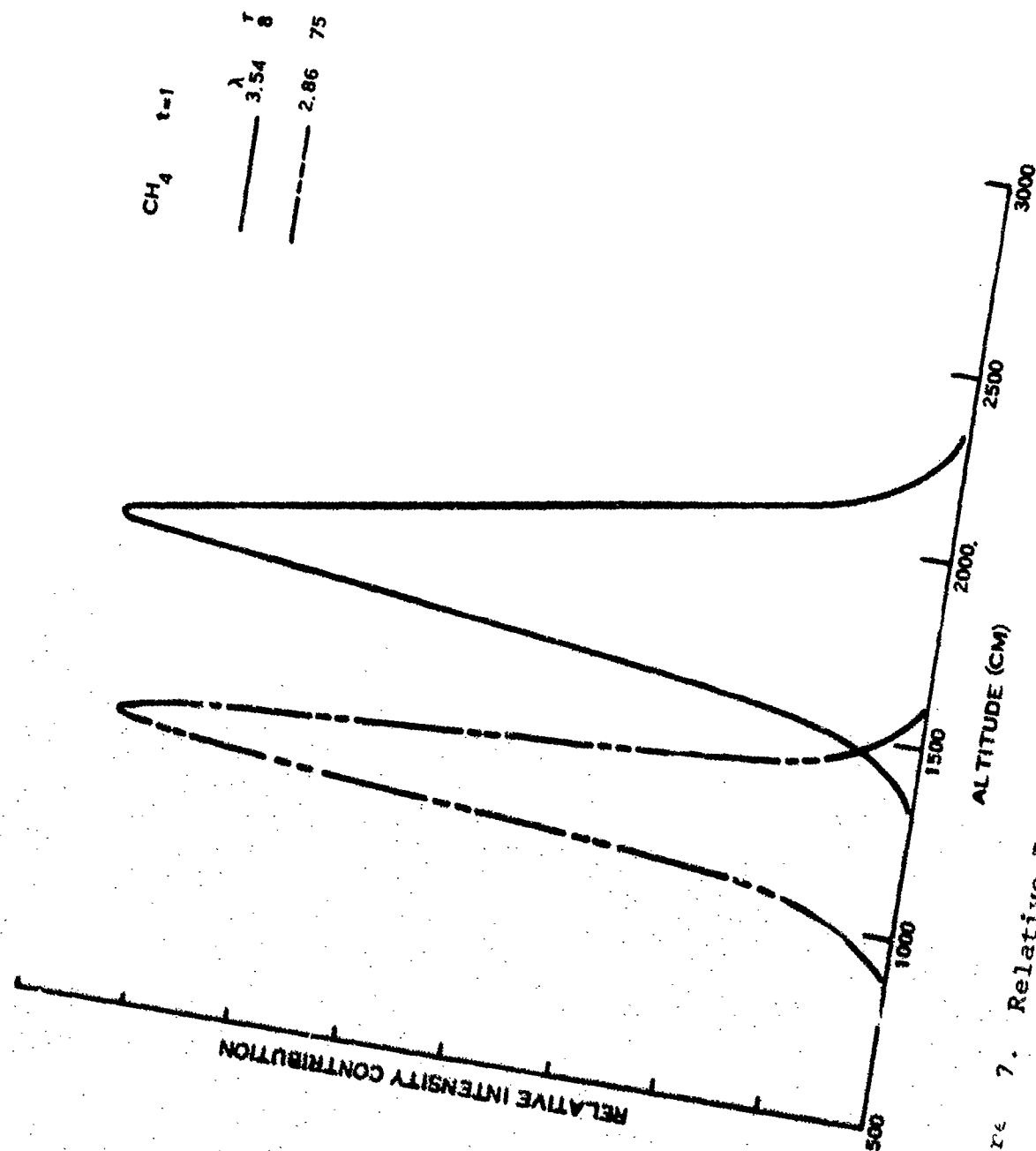
25

Figure 7. Relative Intensity Contribution Profiles for CH_4/O_2 Explosion. Time = 1 Second.
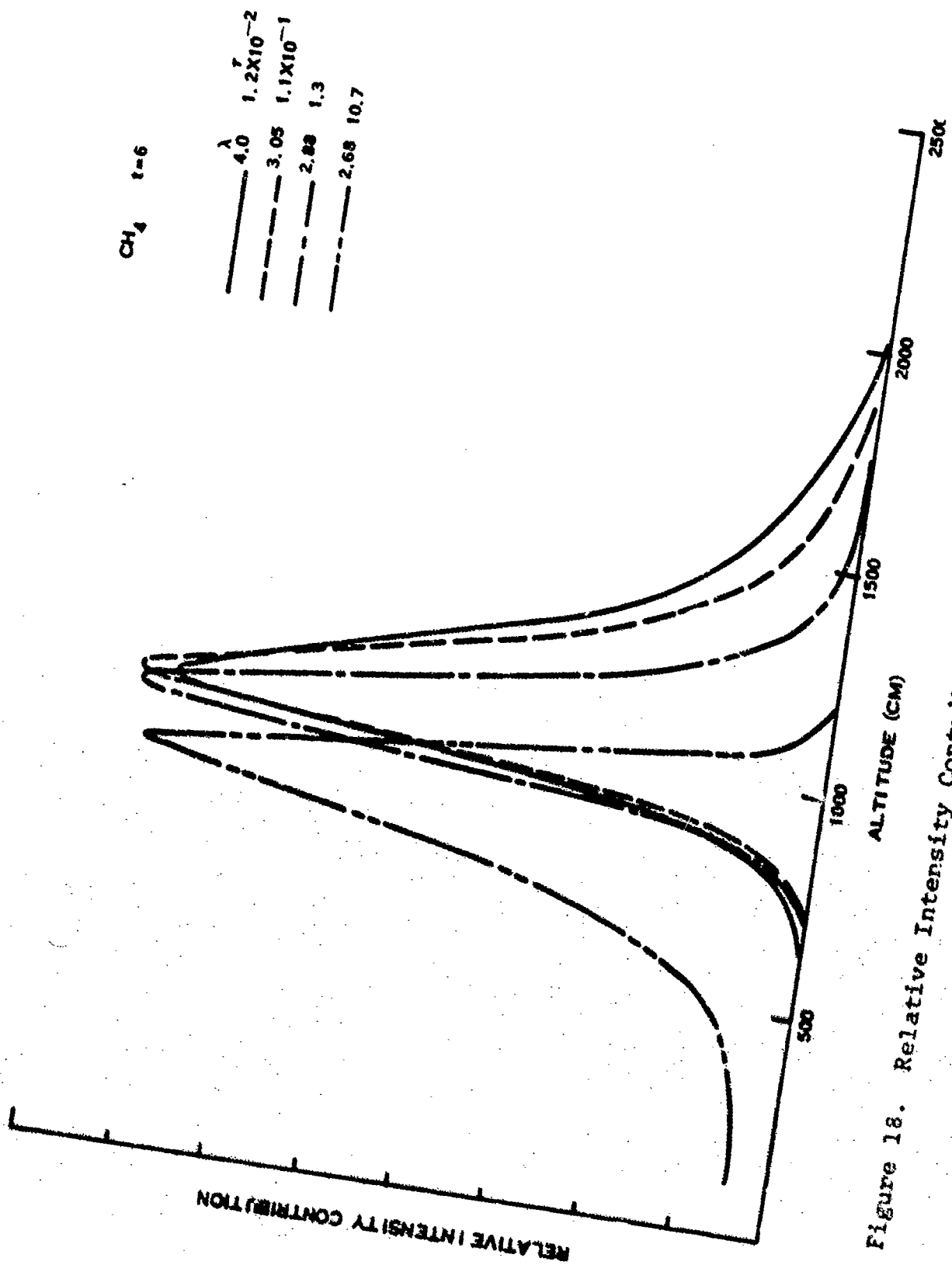
Figure 18. Relative Intensity Contribution Profiles for CH_4/O_2 Explosion.
Time = 6 Seconds.

location of this region is a function of time and is determined by the optical thickness. The computed intensity does not vary significantly with time. On the other hand, radiation from the wings of the bands originates in the region of the peak temperature, and the intensity is strongly dependent on time.

III.3   EXPERIMENT DESIGN

The prime considerations in the design of the IR vidicon field experiment are data interpretation and dynamic range. Of secondary importance is the observation of seedants or tracers which can be used to follow the entrainment process as was originally suggested by Wolfhard and Alyea.[9] Fortunately, these requirements are compatible in certain wavelength regions, the selection of which is described below.

When the debris cloud is optically thick, absorption determines that spatial region which is observed (see Figure 17). Consequently, optical thickness effects must be removed to obtain the true distribution of temperature and concentrations within the cloud. This correction will depend upon the profiles themselves and complicate data analysis immensely. For this reason, wavelengths where the cloud is always thin should be selected for observation.

Referring to Figure 19, wavelengths below 2.65 microns are optically thin for $CO/O_2/H_2O$ explosions. The debris from CH_4/O_2 mixtures is always optically thick at early times. However, at late times, greater than four seconds, the cloud is optically thin at wavelengths less than 2.45 microns or greater than 3 microns. These ranges then, are ideal from the viewpoint of data interpretation.

The IR vidicons have a dynamic range of approximately 100. Thus, it is not possible to observe the entire event using one sensor system (see Figures 15 and 16). Consequently, it is recommended that the two available vidicon sensors observe the same wavelength range
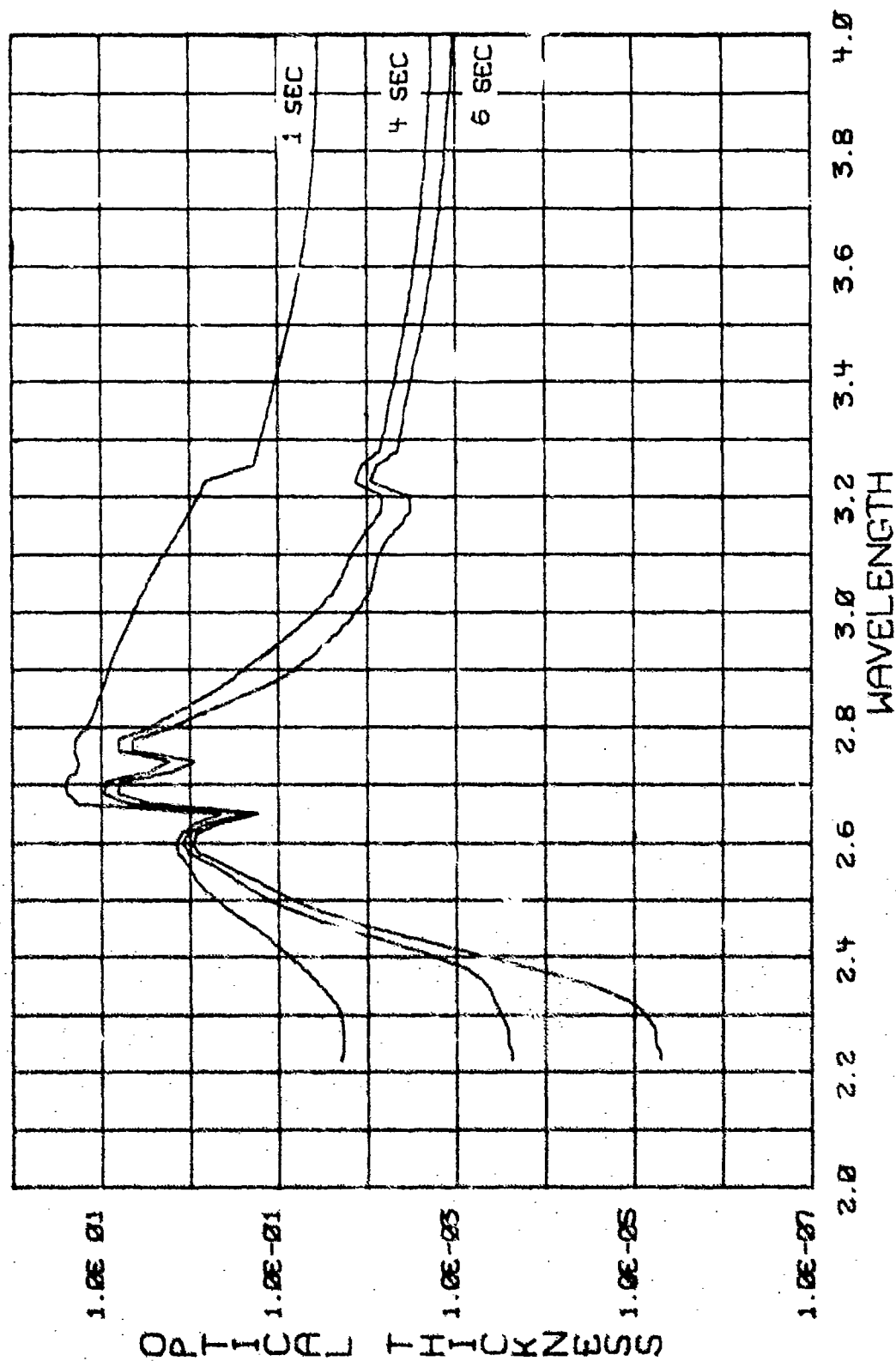
26

Figure 19. Spectral Optical Thickness to Peak Temperature Point for $CO/O_2/H_2O$ Explosions.
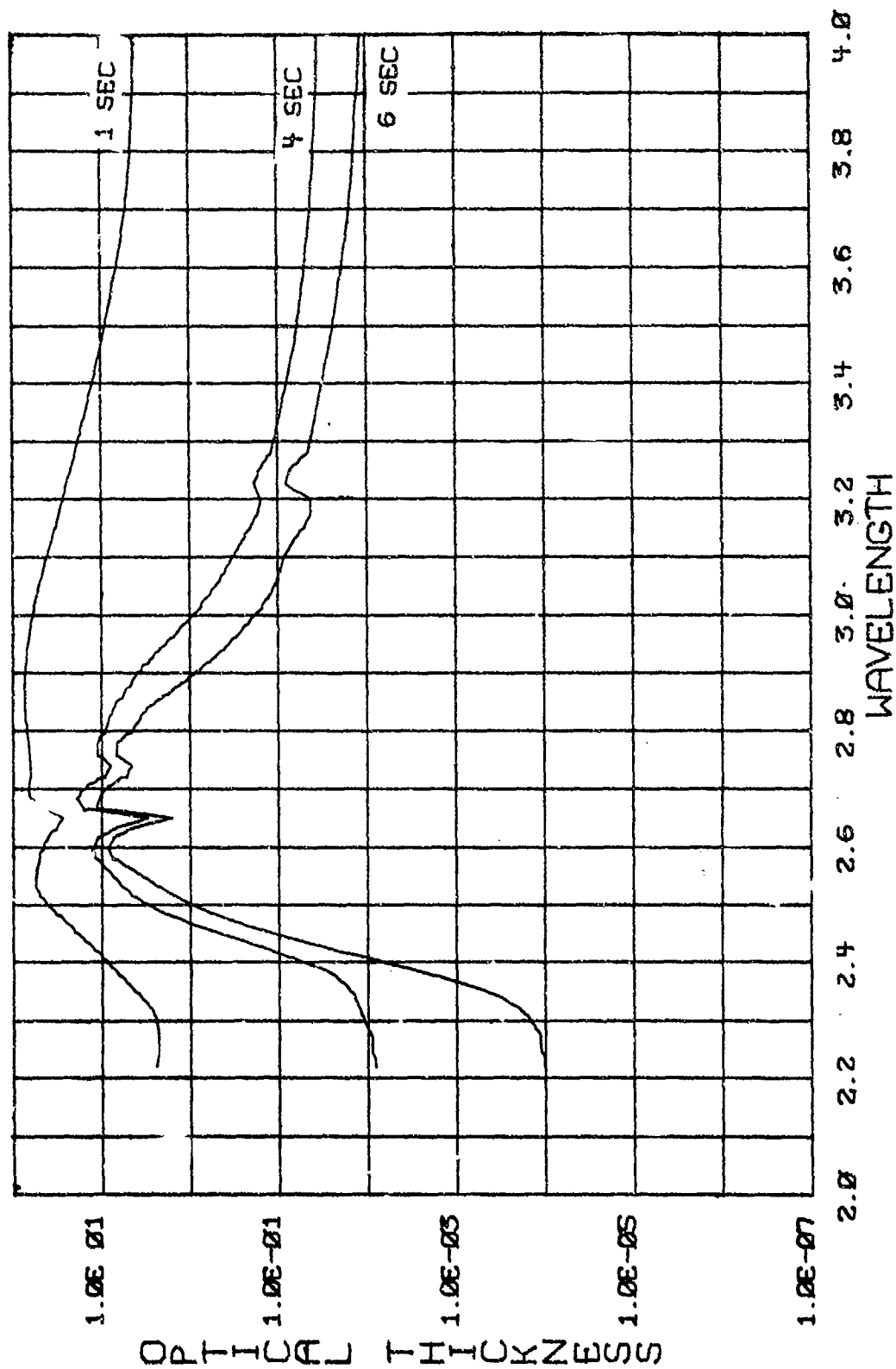
29

Figure 20. Spectral Optical Thickness to Peak Temperature Point for CH_4/O_2 Explosions.

using different sensitivities. This will extend the available dynamic range from 100 to 10.[4] Further, the low gain system which responds to peak, early time intensities will be equipped with a field stop to reduce light levels. After several seconds the intensity of the event will decrease to the noise level of the field stopped system. At this point, the stop will be physically removed and the sensor will operate wide open to provide high gain response. This in effect will increase the available dynamic range to 10^6 which is more than sufficient to cover the intensity variation over the time period of interest for the optically thin spectral regions cited above.

A second difficulty associated with vidicon sensors is the effect of saturation on the less intense regions of the image, i.e., the familiar blooming effect. The predictions presented in this report represent peak intensity levels. The edge of the disturbed region, however, will have an intensity characteristic of the background level. Blooming of the center region then may saturate the entire image and eliminate useful data. Hence, it may be necessary to work in a spectral interval where the intensity of the central region is reduced by absorption while the edges which are thinner are not. This, in effect, will decrease the dynamic range over the image and allow observation of the less intense spatial features. In the case of $CO/O_2/H_2O$ explosions, 2.5 to 2.6 microns is ideal while for CH_4/O_2, 2.9 to 3.0 microns appears a reasonable choice to minimize blooming effects.

The use of seedants or tracers to visualize the fluid mechanical processes is appealing. The proposed experiment would employ small bags or containers of tracer material suspended within the main balloon. Motion of these point sources within the flow should enable elucidation of phenomenon such as entrainment and turbulence. The seeding material must, of course, have an observable IR spectrum. Further, it must be stable under the high temperature conditions of the explosion and remain gaseous as the debris cools.

Of the materials examined, the hydrogen halides are most advantageous.[9] HF emits strongly in the 2.3 to 2.8 micron region while the HCl spectrum is most intense from 3.3 to 3.7 microns. These materials are stable and remain gaseous at low temperature.

Table II summarizes the favorable wavelength region for observing the mixtures under consideration within the limits described above. The results show that all criteria can be achieved for $CO/O_2/H_2O$ mixtures at wavelengths between 2.5 to 2.6 microns. On the other hand, no single wavelength can be selected for CH_4/O_2 mixtures. 2.9 to 3.0 microns will minimize blooming while HCl can be observed only above 3.3 microns. Consequently, the appropriate filter cannot be selected before the extent of the blooming problem is determined in the laboratory.

TABLE II

FAVORABLE WAVELENGTHS FOR OBSERVATION OF EXPLOSION DEBRIS

PROPERTY	MIXTURE	
	$CO/O_2/H_2O$	CH_4/O_2
Optically thin	$<2.65\mu$	$<2.45\mu$*
		$>3.0\mu$
Minimize blooming	$2.5-2.6\mu$	$2.9-3.0\mu$
Observe seedant	HF $2.3-2.8\mu$	HCl $3.3-3.7\mu$

*CH_4/O_2 is always optically thick before 4 seconds.

33

CONCLUSIONS AND RECOMMENDATIONS

Predictions of the IR radiation produced by the debris of stoichiometric $CO/O_2/H_2O$ and CH_4/O_2 mixtures have been made. The calculation considered optical thickness effects as well as spatial and temporal variations of the major species, CO_2 and H_2O and temperature. The results show that the spectral intensity is a strong function of wavelength and is determined in part by the optical thickness of the cloud.

The predictions have been applied to select appropriate filters for an infrared vidicon sensor system which will be used for observation of balloons exploded in the field. The following recommendations are made:

1. The two available vidicon cameras should be operated to provide maximum dynamic range. This can be accomplished by using matched spectral filters and adjusting the sensitivities of the cameras such that they just overlap.

2. $CO/O_2/H_2O$ explosions are preferable to those of CH_4/O_2 because the former are optically thin. This obviates laborous and uncertain corrections for the removal of optical thickness effects.

3. 2.5-2.6 microns is an ideal wavelength for observation of $CO/O_2/H_2O$ mixtures. The debris is always optically thin, the dynamic range over the time period of interest is acceptable and HF can be used as a seedant.

4. Two filters are recommended for CH_4/O_2 mixtures. The first, between 2.9-3.0 microns, will minimize the effect of blooming but, will not be capable of observing a seedant. If laboratory experiments demonstrate that blooming is not significant, a filter at 3.3 microns will be satisfactory and can observe an HCl seedant.

34

REFERENCES

1. Bigoni, R.A., and Matuska, D.A., "Gas Explosive Simulation Technique", AFWL-TR-73-129, May 1973.

2. Fremont, H.A., Powell, H.N., Shaffer, A., and Suciu, S.N., "Properties of Combustion Gases System: C_nH_{2n}-Air", General Electric, ATG Development Dept., Cincinnati, Ohio, 1955.

3. Chandrasekhar, S., Radiative Transfer, Dover, New York, 1960, p. 8.

4. Bortner, M.H., Alyea, F.N., et al, "Development of the Carbon Monoxide Atmospheric Pollution Experiment Phase One Report", GE Document NAS1-10139, 1972.

5. Ferriso, C.C., Ludwig, C.B., and Thomson, A.L., "Empirically Determined Absorption Coefficients of H_2O from 300 to $3000°K$", JQSRT 6, 241, 1966.

6. Malkmus, W., "Infrared Emissivity of Carbon Dioxide (2.7μ Band)", J Opt. Soc. Am. 54,751, 1964.

7. Infrared Physics and Engineering, Jamison, J.J., et al, Mc Graw Hill, 1963, New York, p. 109.

8. Bigoni, R.A., AFWL, private communication, June 1973.

9. Wolfhard, H.A., IDA; and Alyea, F.N., private communication, January 1973.